Hypothyroid Phenotype Is Contributed by Mitochondrial Complex I Inactivation Due to Translocated Neuronal Nitric-oxide Synthase*

María C. Franco[‡], **Valeria G. Antico Arciuch**[‡], **Jorge G. Peralta**[‡], **Soledad Galli**[‡], **Damián Levisman**[‡], **Lidia M. López**[§], **Leonardo Romorini**[¶], **Juan J. Poderoso**[‡], and **María C. Carreras**[‡||1]

From the [‡]Laboratory of Oxygen Metabolism, University Hospital, [§]Instituto de Biología Celular y Neurociencia "Profesor Eduardo de Robertis," Facultad de Medicina, [¶]Departamento de Química Biológica, Facultad de Ciencias Exactas y Naturales, and [||]Departamento de Bioquímica Clínica, Facultad de Farmacia y Bioquímica, University of Buenos Aires, 1120-Buenos Aires, Argentina

Although transcriptional effects of thyroid hormones have substantial influence on oxidative metabolism, how thyroid sets basal metabolic rate remains obscure. Compartmental localization of nitric-oxide synthases is important for nitric oxide signaling. We therefore examined liver neuronal nitric-oxide synthase-α (nNOS) subcellular distribution as a putative mechanism for thyroid effects on rat metabolic rate. At low 3,3′,5-triiodo-L-thyronine levels, nNOS mRNA increased by 3-fold, protein expression by one-fold, and nNOS was selectively translocated to mitochondria without changes in other isoforms. In contrast, under thyroid hormone administration, mRNA level did not change and nNOS remained predominantly localized in cytosol. In hypothyroidism, nNOS translocation resulted in enhanced mitochondrial nitric-oxide synthase activity with low O_2 uptake. In this context, NO utilization increased active O_2 species and peroxynitrite yields and tyrosine nitration of complex I proteins that reduced complex activity. Hypothyroidism was also associated to high phospho-p38 mitogen-activated protein kinase and decreased phospho-extracellular signal-regulated kinase 1/2 and cyclin D1 levels. Similarly to thyroid hormones, but without changing thyroid status, nitric-oxide synthase inhibitor N^ω-nitro-L-arginine methyl ester increased basal metabolic rate, prevented mitochondrial nitration and complex I derangement, and turned mitogen-activated protein kinase signaling and cyclin D1 expression back to control pattern. We surmise that nNOS spatial confinement in mitochondria is a significant downstream effector of thyroid hormone and hypothyroid phenotype.

Hypothyroidism is a prevalent disorder associated to low oxygen utilization and low tissue proliferation rate (1). In addition to non-genomic effects (2), thyroid hormones influence transcription of a number of nuclear and mitochondrial-encoded respiratory genes (3). Although direct or transcriptional effects have considerable impact on oxidative metabolism and hemodynamic function, much is still unknown about how thyroid hormones set the metabolic rate of the body (4); consonant

with slowness of transcriptional mechanisms, treatment of hypothyroidism may require weeks of hormone administration to normalize the altered functions (5). In the last decade, the effects of nitric oxide (NO)[2] expanded from the vascular system to the intracellular milieu. In this context, subcellular localization of nitric oxide-synthases (NOS) with effector molecules is an important regulatory mechanism for NO signaling (6, 7). Accordingly, we are interested in the traffic of a posttranslationally modified variant of neuronal nitric-oxide synthase-α (nNOS) to mitochondria (formerly named mitochondrial nitric-oxide synthase or mtNOS), which vectorially directs NO to the matrix compartment (8, 9). mtNOS could be low in adult rodents, but a modulated increase has been associated to thyroid status (10), release of cytochrome c (11), mitochondrial protein nitration (12), liver and brain development (13, 14), adaptation to cold environment (15), and hypoxia (16).

Under physiological O_2 levels and *in vivo* respiratory dynamics, NO inhibits mitochondrial state 3 and 4 O_2 uptake (17). At 10–20 nM, matrix NO tonically modulates O_2 uptake by reversible inhibition of cytochrome oxidase through heme iron nitrosylation at a-a_3 subunit (18) and promotes the formation of superoxide (O_2^-) and hydrogen peroxide (H_2O_2) (18, 19). At complexes I and II-III, mitochondrial production of O_2 species depends on autoxidation of intermediary ubisemiquinone during electron transfer from reduced ubiquinol pools to cytochrome c_1, with formation of O_2^-. This reaction is considerably amplified by NO inhibition of cytochrome oxidase or cytochrome b-c_1 segment that augments the reduction on the side of substrates (18, 19). In mitochondria, O_2^- is either dismutated to H_2O_2 by manganese superoxide dismutase (Mn-SOD) or reacts with NO to form peroxynitrite (ONOO$^-$). Considering that, variations in matrix NO differently change the proportion of these active species (19); the aim of this work was to search for nNOS traffic to mitochondria and its consequences in O_2 uptake, mitochondrial oxidant yield, and cell responses (13) as experimentally related to thyroid status.

EXPERIMENTAL PROCEDURES

Materials—3,3′,5-triiodo-L-thyronine (T_3), N^G-methyl L-arginine (L-NMMA), N^ω-nitro-L-arginine methyl ester (L-NAME), and LR-White acrylic resin were from Sigma-Aldrich. 2′,7′-dichlorofluorescein diacetate (DCFH-DA), hydroethidine (HE), 4-amino-5-methyl-

2 The abbreviations used are: NO, nitric oxide; nNOS, eNOS, iNOS, and mtNOS, neuronal, endothelial, inducible, and mitochondrial nitric-oxide synthase; BMR, basal metabolic rate; T_3, 3,3′,5-triiodo-L-thyronine; Mn-SOD, manganese superoxide dismutase; CAT, catalase; GPX, glutathione peroxidase; L-NAME, N^ω-nitro-L-arginine methyl ester; Hsp, heat shock protein; MAPK, mitogen-activated protein kinase; ERK, extracellular signal-regulated kinase; L-NMMA, L-N^G-methyl-L-arginine.

amino-2′,7′-difluorescein diacetate (DAF-FM), MitoTracker Red 580, SYBR Green, and 39-kDa subunit of Complex I and VIc subunit of Complex IV monoclonal antibodies were from Invitrogen-Molecular Probes. Leukemia virus reverse transcriptase (MMLV-RT) and *Taq* polymerase were from Promega Corp. (Madison, WI). MAPK antibodies were from Cell Signaling Technology (Beverly, MA). Monoclonal nitrotyrosine antibody was provided by Prof. Alvaro Estévez, University of Alabama at Birmingham. Monoclonal nNOS and polyclonal eNOS antibodies were from BD Transduction Laboratories. Polyclonal nNOS, iNOS, Hsp90, and cyclin D1 antibodies were from Santa Cruz Biotechnology Inc. (Santa Cruz, CA). Methimazole was provided by Laboratorios Gador (Buenos Aires, Argentina).

Animals and Treatments—Male Wistar rats (250–300 g) were housed in a temperature-controlled room with food and water *ad libitum*; National Institutes of Health criteria for animal research were followed after approval by the Ethics Committee of the University Hospital. Rats were divided into five groups ($n = 12$/group): hypothyroid, (0.02% methimazole (w/v) in drinking water for 28 days); hypothyroid+T_3, (after 25 days of methimazole treatment received 15 μg of T_3/kg of body weight for 3 days by intraperitoneal injection); hypothyroid+L-NAME, (0.75 mg/ml L-NAME in drinking water in the last 21 days of methimazole treatment); hyperthyroid, (intraperitoneal injection of 60 μg of T_3/kg of body weight for 3 days); and control group. Blood samples were collected at the time the animals were killed for estimation of thyrotropin (TSH) level by radioimmunoassay (20).

Basal Metabolic Rate—BMR was measured at 22 °C in a non-recirculating open flow system after 30 min of equilibration with an O_2-CO_2 analyzer in standard temperature and pressure dry conditions (15).

Isolation and Purification of Liver Mitochondria—The livers were excised in ice-cold homogenization medium, and mitochondria were isolated and purified as described (13). Minimal contamination was found (2–3%) by comparing activities of lactate dehydrogenase (cytosolic marker) and succinate-cytochrome *c* reductase (mitochondrial marker).

RT-PCR—Total liver RNA was extracted with TRIzol, and RT-PCR was performed (21). Primers for β2-microglobulin and NOS isoforms were as described (21–23): for cyclin D1, sense (5′-GCGTACCCTGA-CACCAATCT-3′) and antisense (5′-GCTCCAGAGACAAGAAACG-G-3′). Nested PCR for eNOS isoform (35 cycles) was done with 0.5 μl of PCR product in 30-μl final volume with inner primers, sense (5-ATG-TGGCTGTCTGCATGGAT-3′) and antisense (5′-TTGCTGCACTT-CTTTCCAG-3′).

Quantitative Real-time PCR—Real-time nested PCR for nNOS isoform was done with 0.5 μl of a 1/10 dilution of PCR product in 25-μl final volume with inner primers: nNOS, sense (5′-TTCAACTA-CATCTGTAACCA-3′) and antisense (5′-TGAACTGCACATTG-GCTGGA-3′). Real-time PCR reactions included 0.4 mM dNTPs, 1 μM specific primers, 4 mM $MgCl_2$, 2.5 units of *Taq* DNA polymerase, and 1:30,000 SYBR Green. Real-time PCR reactions were performed in DNA Engine Opticon (MJ Research, Inc.) and consisted of an initial denaturing step (94 °C for 4 min), followed by 35 cycles (each of 94 °C for 1 min, 55 °C for 40 s, 72 °C for 1 min). Sample quantification was normalized to endogenous β2-microglobulin that was also quantified by real-time PCR following the same protocol as nNOS isoform. Each experiment included a DNA minus control and a standard curve.

Immunoblotting for NOS, Hsp90, and Mitochondrial Protein Nitration—Proteins were electrophoresed on 7.5% SDS-polyacrylamide gel, electrotransferred to polyvinylidene difluoride membranes (13), incubated with anti-nNOS, anti-eNOS, anti-iNOS, anti-Hsp90, and anti-nitrotyrosine antibodies, and detected with the ECL system. Equal loading was controlled with the appropriated subcellular markers. Incu-

bation of the anti-nitrotyrosine antibody with 10 mM nitrotyrosine prior to the membrane incubation was used to ensure the antibody specificity.

NOS Activity in Subcellular Fractions—NOS activity was determined in mitochondrial and cytosolic fractions by conversion of [^{3}H]L-arginine to [^{3}H]L-citrulline (13).

Immunoelectron Microscopy—Purified mitochondria were suspended in 4% paraformaldehyde and 0.5% glutaraldehyde, pH 7.4, for 2 h at 4 °C, washed overnight with 0.32 M sucrose at 4 °C, and then dehydrated in 70% ethanol and embedded in LR White (13). Ultrathin sections were obtained in 300-mesh nickel grids. Immunocytochemistry was performed using a primary mouse anti-C-terminal nNOS (1095–1289) at a dilution of 1:20 in phosphate-buffered saline, pH 7.4. Grids were washed in phosphate-buffered saline and counterstained with 1% uranyl acetate. Nonspecific background was blocked by incubation with 5% normal goat serum in phosphate-buffered saline at the beginning of the procedure. Positive control against 39-kDa subunit of complex I (inner membrane marker) and negative control in the absence of a primary antibody were included. Specimens were observed in a Zeiss EM-109-T transmission electron microscope at 80 kV.

Detection of Mitochondrial NO—Mitochondria (1 mg of protein per ml) were incubated in phosphate-buffered saline for 30 min at 37 °C with 5% CO_2, 10 μM DAF-FM, and 0.5 μM MitoTracker, and fluorescence was measured with an Ortho-Cytoron Absolute Cytometer (Johnson and Johnson) (24).

Mitochondrial O_2 Utilization and Electron Transfer Activity—O_2 uptake was measured polarographically with a Clark-type electrode (10). To assess NO effects, mitochondria were incubated with 0.3 mM L-arginine (L-Arg) alone or plus 3 mM L-NMMA for 5 min at 37 °C (10). State 4 O_2 uptake was determined with 6 mM malate-glutamate as substrate of complex I and state 3 active respiration by the addition of 0.2 mM adenosine diphosphate (ADP). Complex I activity (NADH: ubiquinone reductase) was measured by the rotenone-sensitive reduction of 50 μM 2,3-dimethoxy-6-methyl-1,4-benzoquinone with 1 mM KCN and 200 μM NADH as electron donor at 340 nm with a Hitachi U3000 spectrophotometer at 30 °C. Activity of complexes II-III was determined by cytochrome *c* reduction at 550 nm. Cytochrome oxidase activity (Complex IV) was determined by monitoring cytochrome *c* oxidation at 550 nm (ϵ_{550}, 21 mM^{-1}·cm^{-1}); the reaction rate was measured as the pseudo-first order reaction constant (k') and expressed as k'/min·mg of protein (13, 14).

Mitochondrial Production of H_2O_2 and O_2^-—H_2O_2 production rate was monitored spectrofluorometrically at complexes I or II-III (6 mM malate-glutamate or 10 mM succinate as substrate) in an F-2000 spectrofluorometer (Hitachi, Tokyo, Japan) as described (13). To determine O_2^- at complexes I and II-III, mitochondria were subjected to three freeze/thaw cycles, and SOD-sensitive cytochrome *c* reduction was measured at 550 nm (0.1 mg of protein/ml and 10 μM SOD to subtract unspecific reduction). Mn-SOD, catalase, and glutathione peroxidase activities were determined in 7,000 *g* supernatants as described (13).

Liver Cell Isolation and Detection of Intracellular Oxidants—Hepatocytes were isolated by two-step collagenase perfusion (25). Intracellular oxidants and mitochondrial (O_2^-) were detected by flow cytometry after incubating hepatocytes in phenol red-free Dulbecco's modified Eagle's medium with 5 μM DCFH-DA or 5 μM HE for 30 min at 37 °C with 5% CO_2.

Blue Native Polyacrylamide Gel Electrophoresis—To separate mitochondrial complexes, Blue Native-PAGE was performed according to Schägger (26). Gels of first dimension were stained with Coomassie Blue and membranes incubated with antibodies against 3-nitrotyrosine. For second-dimension analysis, gel bands, corresponding to the complex I

TABLE 1

Oxygen uptake rates depend on thyroid status and nitric oxide utilization

Data are mean ± S.E. of the different groups (n = 5–6 animals/group). O_2 uptake rate and complex activities were measured in intact mitochondria and mitochondrial membranes, respectively. *, different from controls; †, different from L-NMMA, by analysis of variance and Dunnett *post hoc* test. To avoid effects of body weight on resting metabolic rate, O_2 uptake was corrected to lean body mass and exponentially related to mass$^{0.75}$. ngat, nanogram atom.

	Control	Hypothyroid	Hypothyroid + T$_3$	Hyperthyroid
TSH *(ng/ml)*	12 ± 2	>80*	11 ± 2	5 ± 1*
Basal metabolic rate *(ml of O_2/min·kg$^{0.75}$)*	17 ± 1	12 ± 1*	18 ± 1	23 ± 1*
Mitochondrial $O_{2\ uptake}$ *(ngat/min·mg of protein)*				
State 4 uptake				
Basal	14.2 ± 1.3	11.5 ± 1.7	15.8 ± 1.7	16.9 ± 0.3
+ 0.3 mM L-Arg	13.8 ± 0.7	9.0 ± 0.5 †	14.0 ± 1.7	14.8 ± 0.6
+ 3 mM L-NMMA	15.6 ± 0.8	12.4 ± 2.0	14.6 ± 1.8	16.2 ± 2
State 3 uptake				
Basal	79 ± 6	49 ± 3*†	89 ± 5	102 ± 10
+ 0.3 mM L-Arg	72 ± 7	46 ± 2†*	85 ± 5	106 ± 10*
+ 3 mM L-NMMA	86 ± 8	62 ± 4*	92 ± 5	105 ± 8
Calculated matrix (NO) *(nM)*	23 ± 9	94 ± 7	54 ± 15	6 ± 3
Enzyme activities				
Complex I *(nmole/min·mg of protein)*	108 ± 16	41 ± 15*	85 ± 9	98 ± 9
Complex II/III *(nmole/min·mg of protein)*	66 ± 19	62 ± 20	63 ± 16	69 ± 1
Complex IV *(k'/min·mg of protein)*	13.7 ± 0.3	12.3 ± 0.2*	13.5 ± 0.4	14.6 ± 0.4

region derived from 5-mm-wide lanes, were excised and incubated for 2 h in cathode buffer (50 mM glycine and 7.5 mM imidazole, pH 7) supplemented with 1% SDS and 1% β-mercaptoethanol before electrophoresis on 10%-16.5% Tris/glycine gels (27). Membranes were incubated with antibodies against 3-nitrotyrosine.

Immunoprecipitation—For immunoprecipitations, 500 μg of mitochondrial proteins were incubated with 4 μg of antibodies against Complex I 39-kDa subunit or Complex IV VIc subunit and 30 μl of Protein A/G PLUS-agarose (Santa Cruz) at 4 °C; samples were blotted against polyclonal nNOS antibody. Protein loading was controlled by the respective mitochondrial complex antibodies.

Preparation of Whole Liver Homogenates and Immunoblotting for MAPKs and Cyclin D1—To study MAPKs and cyclin D1, liver was homogenized in lysis buffer as described (13). Proteins were separated on 12% SDS-PAGE, and cyclin D1 and MAPKs were detected with specific antibodies.

Metabolic Calculations—All experiments were done at 1 mg of mitochondrial protein per ml (n = 5). Mitochondrial H_2O_2 steady-state concentration ($[H_2O_2]_{ss}$) was calculated according to Ref. 13 as shown in Equation 1.

$$[H_2O_2]_{ss} = \ + d[H_2O_2]/dt/k_1 \times [CAT] + k_2 \times [GPX] \quad \text{(Eq. 1)}$$

where $+ d[H_2O_2]/dt$ is the rate of L-arginine-dependent H_2O_2 production in Ms^{-1} (Fig. 2*A, upper panel*), $k_1 = 4.6 \times 10^7$ M^{-1} s^{-1}, and $k_2 = 5 \times 10^7$ M^{-1} s^{-1} · CAT and GPX correspond to catalase and glutathione peroxidase concentrations determined spectrophotometrically as previously described (13).

Mitochondrial (O_2^-) steady-state concentration ($[(O_2^-)]_{ss}$) was calculated from Equations 2 and 3 as follows.

$$^1/_2 d[H_2O_2]/dt = -d[O_2^-]/dt$$
$$-d[O_2^-]/dt = k_3[O_2^-][SOD] + k_4[O_2^-][NO] \quad \text{(Eq. 2)}$$

$$[O_2^-]_{ss} = \frac{^1/_2 d[H_2O_2]/dt}{k_3[SOD] + k_4[NO]} \quad \text{(Eq. 3)}$$

k_3 and k_4 are, respectively, 2.3×10^9 and 1.9×10^{10} M^{-1} s^{-1}, and [SOD] was determined spectrophotometrically by inhibition of cytochrome *c* reduction (13).

Matrix NO ($[NO]_{ss}$) was calculated by the percentage of liver mitochondria state 3 respiratory rate NO-dependent inhibition as previously described (15, 19). [ONOO$^-$] production rate was calculated as shown in Equation 4.

$$d[ONOO^-]/-dt = k_4[NO][O_2^-] \quad \text{(Eq. 4)}$$

Statistical Analysis—Data are mean ± S.E. One-way analysis of variance was utilized with *post hoc* Dunnett test, and regression analysis and significance were accepted at $p < 0.05$.

RESULTS

At low T$_3$, Transcriptional Increase of nNOS Enhances mtNOS Content—Thyroid status was discriminated by thyrotropin and BMR measurements (Table 1). In this context, nNOS mRNA, protein expression, and activity were clearly modulated by T$_3$ levels (Fig. 1, *A*–*E*). Likewise, nNOS mRNA expression quantified by RT real-time PCR was >3-fold increased in hypothyroid liver compared with controls (Fig. 1*B*), whereas eNOS or iNOS mRNA did not change (data not shown). In addition, nNOS became distinctively enhanced in mitochondria (mtNOS), indicating a subsequent import of the overexpressed enzyme to the organelles; these findings were reverted by hormone replacement (Fig. 1*C*). To corroborate subcellular distribution in the groups, liver fractions were compared. Western blotting confirmed the increase of total nNOS expression represented by liver homogenates and the enrichment of the mitochondrial fraction in the hypothyroid group. Differentially, at high T$_3$, nNOS expression had results similar to controls, but this condition retained the protein predominantly localized in cytosol (Fig. 1*C*). This effect was parallel to the increased expression of heat shock protein 90 (Hsp90), one of the most important chaperones associated to nNOS (Fig. 1*F*). Alternatively, modulation of mtNOS content in the studied groups was validated as well by immunoelectron microscopy with monoclonal nNOS antibodies (Fig. 1*D*). In agreement, Ca^{2+}-dependent NOS activity was significantly increased in hypothyroid mitochondria but was normal to slightly reduced after T$_3$ admin-

FIGURE 1. **NOS changes with thyroid status.** Liver nNOS expression and subcellular distribution are shown at different T_3 levels. *A*, representative RT-PCR for nNOS normalized by stable $\beta2$-microglobulin. *Bars* on the right summarize mRNA variations. *B*, RT quantitative real-time PCR for nNOS. *C*, representative Western blot of proteins separated by SDS/PAGE reveals the differential distribution of cytosol and mitochondrial nNOSα. On the right, comparison of the expression of nNOS in homogenates, cytosol, and mitochondria. Rat brain cytosol is used as nNOS positive control. Protein contents were normalized by specific subcellular markers, subunit VIc of complex IV expression for mitochondria and β-actin expression for cytosol. *D*, immunoelectron microscopy of control and hypo- and hyperthyroid mitochondria against nNOS monoclonal antibodies; positive control with anti-mitochondrial complex I antibody and negative control in the absence of primary antibody are at the *bottom* (original magnification $\times40,000$). *E*, Ca^{2+}-dependent NOS activity was determined in the fractions by [^{3}H]citrulline assay ($n = 8–10$/group). *F*, thyroid effects on Hsp90 expression in cytosol. *, $p < 0.05$ *versus* controls by analysis of variance and Dunnett test.
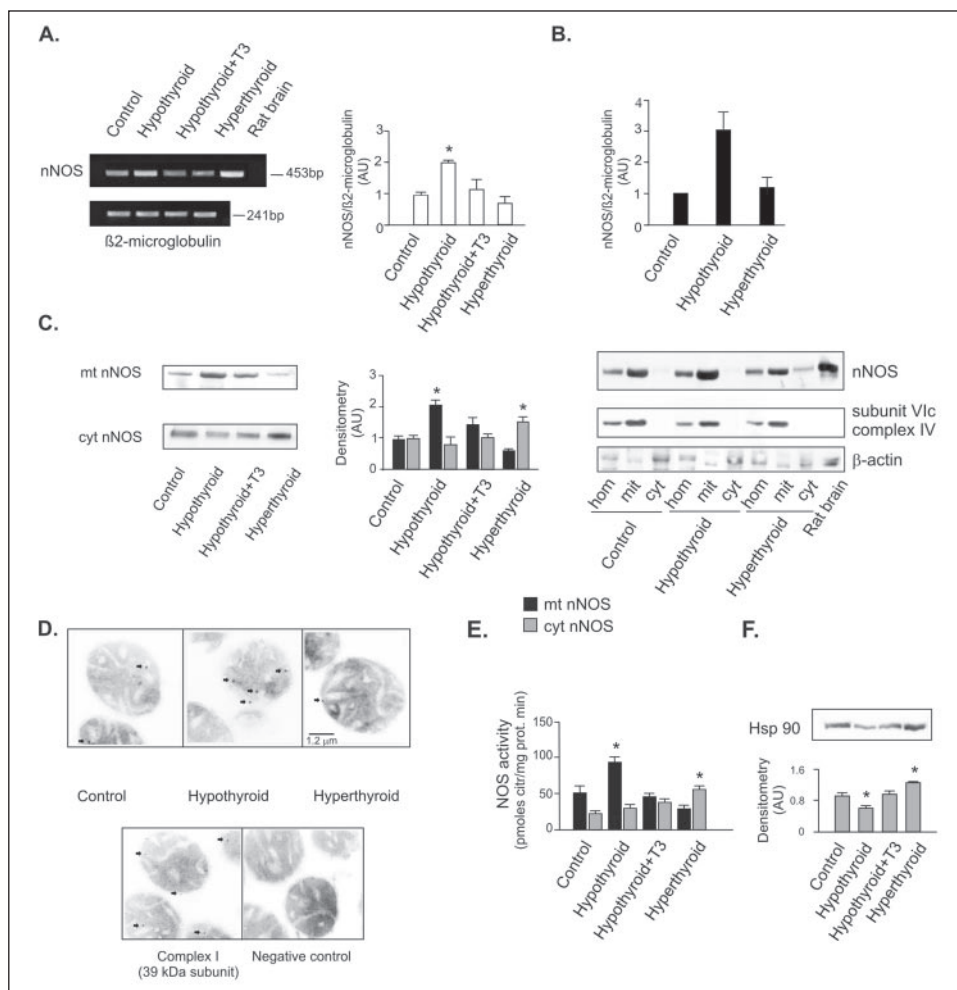
istration, with an opposite cytosolic pattern (Fig. 1*E*); Ca^{2+}-independent NOS activity was not detected.
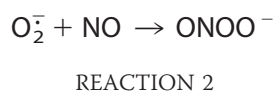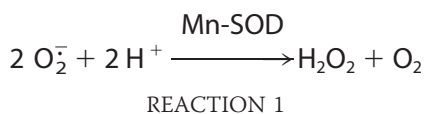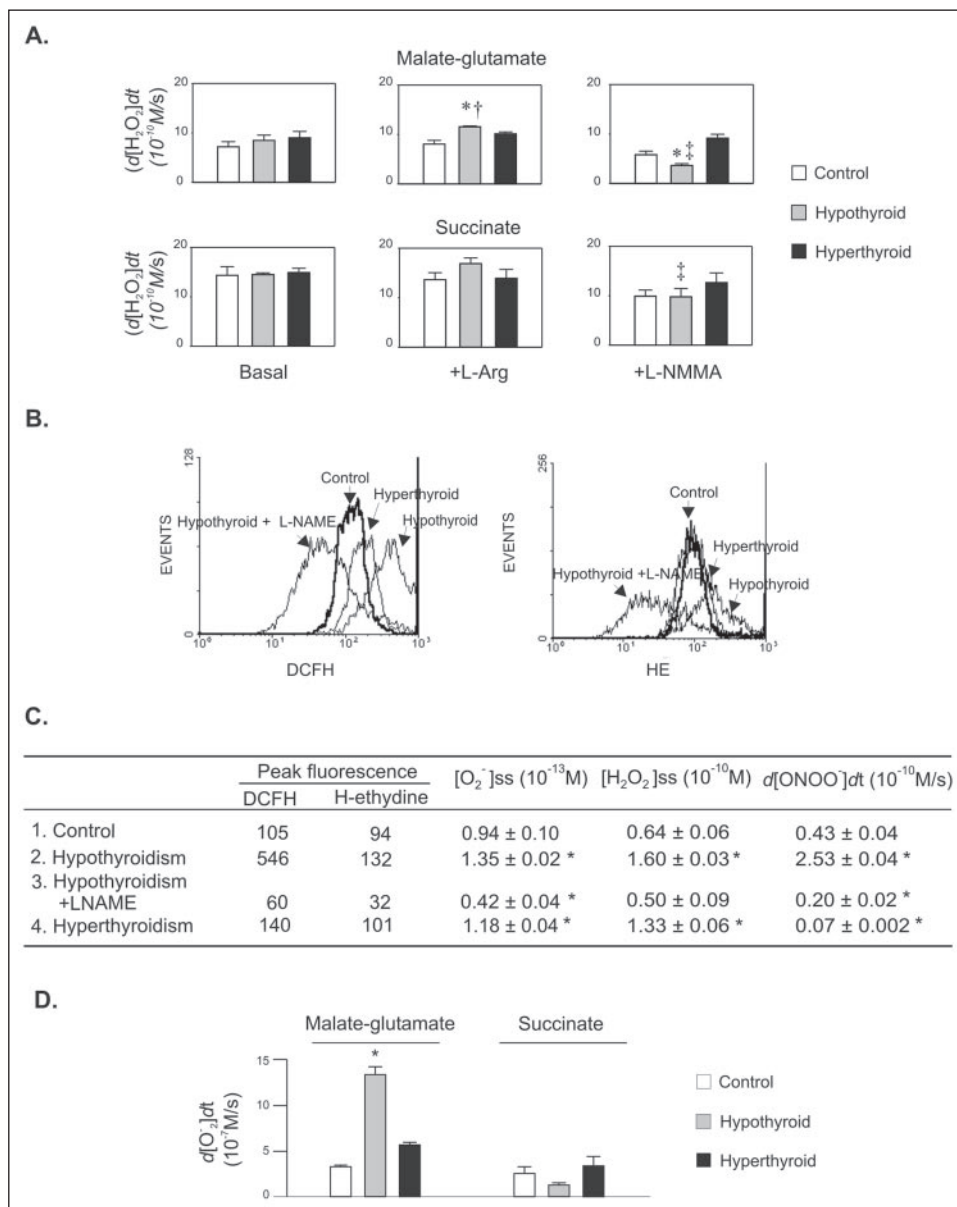
Subcellular nNOS Localization Modulates Mitochondrial Respiration—According to BMR, organelles from hypo- and hyperthyroid groups had the lowest and highest O_2 uptake rates, respectively (Table 1). To discern the effects of mtNOS, mitochondria were supplemented with L-Arg alone or plus NOS inhibitor L-NMMA. The sum of the opposite effects of NOS substrate and inhibitor on basal O_2 utilization determines mtNOS functional activity on respiration (28). Likewise, mtNOS-dependent inhibition of state 3 O_2 uptake was increased ~39% in hypothyroid samples, 18% in controls, and negligible in T_3-treated mitochondria. In agreement, matrix NO estimated from L-Arg inhibition of O_2 uptake (18) was augmented by 4-fold in hypothyroidism and decreased by a half in hyperthyroidism (Table 1). These results demonstrate that (*a*) translocated nNOS is functionally active and mitochondria retain *ex vivo* the cofactors for catalytic activity and (*b*) NOS confinement to the small mitochondrial compartment amplifies NO effects on O_2 uptake and BMR.

We next examined the contribution of segmental activities to mitochondrial O_2 uptake. Electron transfer rate at complex I was markedly decreased at hypothyroid status solely (~ 60%), whereas cytochrome oxidase was less inhibited (~ 11%), and complex II-III activity was not modified (Table 1). No significant thyroid effects on antioxidant Mn-SOD, catalase, or glutathione peroxidase activities were detected.

Thyroid Status Defines Quality and Intensity of Mitochondrial Oxidant Production—In connection with O_2 uptake rate, previous observations proposed a decreased mitochondrial H_2O_2 yield in rat hypothyroidism and an increased yield in hyperthyroidism (29), though opposite results were reported as well (30, 31). It is shown here that basal production of H_2O_2 with substrates of complex I (malate-glutamate) or II (succinate) is not essentially modified by thyroid status (Fig. 2*A*). In contrast, L-Arg enhances the production of mitochondrial active oxygen species from hypothyroid rats, particularly when incubated with malate-glutamate, and L-NMMA prevents its effect. Furthermore, in the presence of L-NMMA, mitochondrial generation of H_2O_2 in hypothyroidism is below that seen in control and hyperthyroid groups, probably because of its reduced number of functional respiratory chain units. Therefore, mtNOS functional activity on H_2O_2 production (calculated by the ratio of NO-dependent to maximal H_2O_2 production in the presence of rotenone (13)), was 33% in hypothyroid mitochondria and 9% in controls. Repercussion of this mitochondrial activity on total cell oxidants *in vivo* is shown in Fig. 2*B*. Hypothyroid-isolated hepatocytes exhibited 30% more HE fluorescence and 280% more DCFH fluorescence than T_3-treated cells, and administration of L-NAME to hypothyroid animals turned oxidant levels down (Fig. 2, *B* and *C*).

Considering that mitochondria and cell O_2^- and H_2O_2 steady-state concentrations depend on two O_2^--utilizing reactions as shown in Reactions 1 and 2,

FIGURE 2. **Cell oxidants follow mitochondrial NO utilization at different T_3 levels.** *A*, H_2O_2 production rate ($d[H_2O_2]/dt$) of purified liver mitochondria at state 4 O_2 uptake ($n = 4 – 8$ rats/group) is plotted in the absence or the presence of 0.3 mM L-Arg alone or plus 3 mM NOS inhibitor L-NMMA, with malate-glutamate or succinate. *B*, representative flow cytometry histograms of isolated hepatocytes incubated in Dulbecco's modified Eagle's medium containing 0.4 mM L-Arg with DCFH-DA or HE were obtained by duplicate, at 504 and 518 nm (excitation) and 529 and 605 nm (emission) respectively. L-NAME was administered to rats as detailed under "Experimental Procedures." *C*, mean of peak fluorescence values of flow cytometry histogram replicates are compared with O_2 species and ONOO⁻ steady-state concentrations calculated from experimental data (see "Experimental Procedures"). *D*, maximal O_2^- production rate was determined by following SOD-sensitive reduction of cytochrome *c*. *, $p < 0.05$ with respect to control; †, idem to basal; ‡, idem to L-Arg.

$$2\,O_2^- + 2\,H^+ \xrightarrow{\text{Mn-SOD}} H_2O_2 + O_2$$

REACTION 1

$$O_2^- + NO \rightarrow ONOO^-$$

REACTION 2

it is then deduced on experimental findings and calculations (Fig. 2*C*) that (*a*) at hypothyroid status, increase of O_2^- and H_2O_2 yields depends on high NO concentration; (*b*) at high NO, O_2^- is also driven to mitochondrial ONOO⁻ formation; (*c*) consequently, *in vivo* DCFH fluorescence is contributed by both H_2O_2, and ONOO⁻ (32); and (*d*) in hyperthyroidism, mitochondrial oxidant production should solely depend on O_2 uptake rate. In accord with low complex I activity, inhibition of electron transfer with cyanide-myxothiazole, which mimics NO inhibitory effects on cytochromes *c*1 and *a-a*3, markedly enhanced O_2^- production rate at complex I in hypothyroidism (Fig. 2*D*).

Nitrative Stress in Hypothyroidism—In relation to expected NO, O_2^-, and ONOO⁻ yields, mitochondria from hypothyroid animals had higher 3-nitrotyrosine content than organelles from the other groups (Fig. 3*A*). In particular, complex I was markedly nitrated on tyrosine, whereas complex IV was nitrated to a lesser extent (Fig. 3*B*). Two-dimensional SDS-PAGE of complex I confirmed an increased nitration of different nuclear and mitochondrial-encoded subunits in hypothyroidism (*MW* suggests nitration in the region of 75, 50 (ND5), 39 (ND4), 30 (ND1), 22 (PDSW), and 17 kDa (B17;18). Control samples showed a constitutive nitration in some of these components, and hyperthyroid samples presented the lowest nitration. In addition, immunoprecipitation of complex I and IV proteins indicated a direct interaction with translocated nNOS, either in control or hypothyroid group (Fig. 3*C*).

NOS Inhibitor L-NAME Prevents Low T_3-dependent Phenotypic Changes—To test whether NOS inhibition prevents T_3 effects on mitochondria, L-NAME was administered to hypothyroid rats. L-NAME neither modified nNOS mRNA (not shown) nor affected nNOS expression or distribution (Fig. 4*A*). Mitochondrial DAF fluorescence (representa-
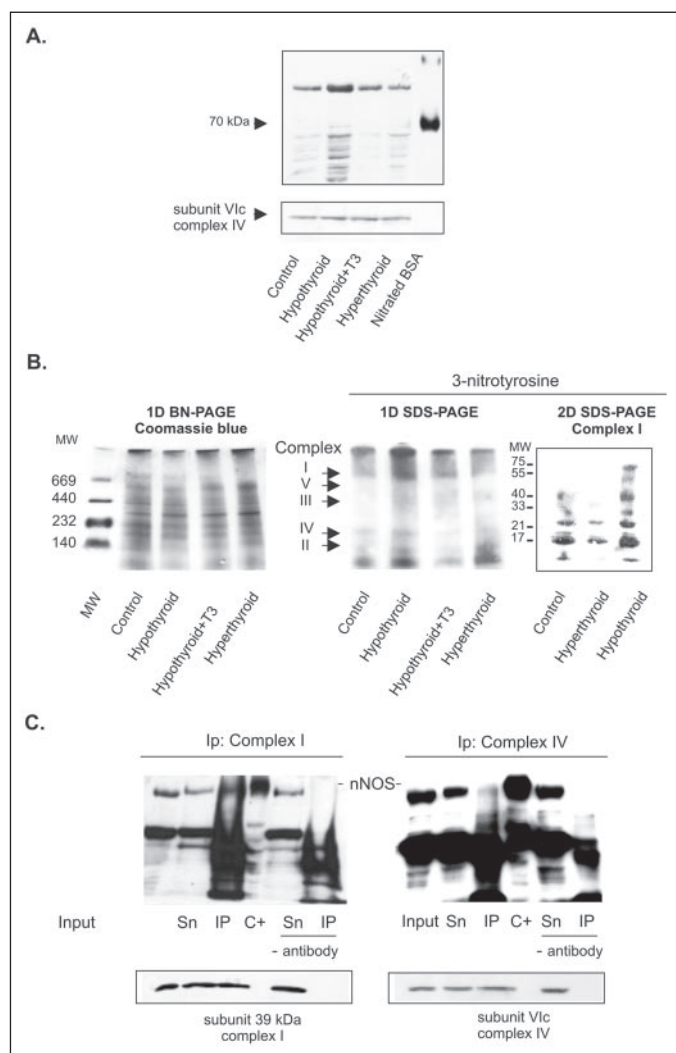
FIGURE 3. **At high mtNOS, hypothyroidism promotes nitration of mitochondrial proteins.** *A*, proteins from the different groups were separated by SDS-PAGE, and membranes were revealed with anti-3-nitrotyrosine antibody; nitrated bovine serum albumin was utilized as positive control. *B*, mitochondrial complexes were separated in Blue Native-PAGE stained with Coomassie Blue (*left*) or transferred to polyvinylidene difluoride membranes and blotted with a polyclonal anti-3-nitrotyrosine antibody (*middle*). Two-dimensional SDS-PAGE of complex I band was blotted against anti-3-nitrotyrosine antibody (*right*) (see "Experimental Procedures"). *C*, mitochondrial proteins from the hypothyroid group were immunoprecipitated with anti-39-kDa subunit (complex I) and anti-subunit VIc (complex IV) antibodies, and immunoprecipitates were subjected to Western blotting with nNOS antibodies. *Input*, purified mitochondria; *Sn*, supernatant; *IP*, immunoprecipitate; *C+*, rat brain cytosol.

FIGURE 4. **NOS inhibitor L-NAME prevents hypothyroid mitochondrial phenotype.** *A*, similar mtNOS content of liver mitochondria from controls and hypothyroid rats treated or not with L-NAME is revealed with anti-nNOS antibody. *B*, representative flow cytometry histogram of 1 mg/ml of isolated mitochondria incubated with 10 μM DAF-FM and 0.5 μM MitoTracker (per duplicate) at 495 nm (excitation) and 515 nm (emission). *C*, a decrease of mitochondrial protein nitration by L-NAME is detected in the hypothyroid condition with anti-3-nitrotyrosine antibody. *D*, inhibition of NOS activity by L-NAME prevented in parallel the hypothyroid lowering of basal metabolic rate (*BMR*) and mitochondrial complex I activity (*n* = 4). *, *p* <0.05 compared with control by analysis of variance. †, idem compared with hypothyroid without L-NAME.

tive of matrix NO) rose by 2-fold at hypothyroidism but decreased to only 25% of this value after L-NAME treatment (Fig. 4*B*). Therefore, at similar thyrotropin levels (>80 ng/ml) and mtNOS content, L-NAME prevented NO increase and nitration of mitochondrial proteins (Fig. 4*C*) and decrease of complex I activity. Accordingly, L-NAME increased BMR of hypothyroid rats up to control values (Fig. 4*D*), whereas no detectable effects were seen in control animals. These results are consistent with L-NAME prevention of the increase of mitochondrial $O_2^{\bar{}}$ and oxidants *in vivo* as shown in isolated hepatocytes (Fig. 2*B*).

Mitochondrial NOS Activity Contributes to Thyroid-dependent Cell Signaling—Thyroid status governs liver cell proliferation (33). This effect depends on activation of proliferating cascades and D-cyclins that stimulate the progression of cell cycle from G_0 to G_1. We have previously described t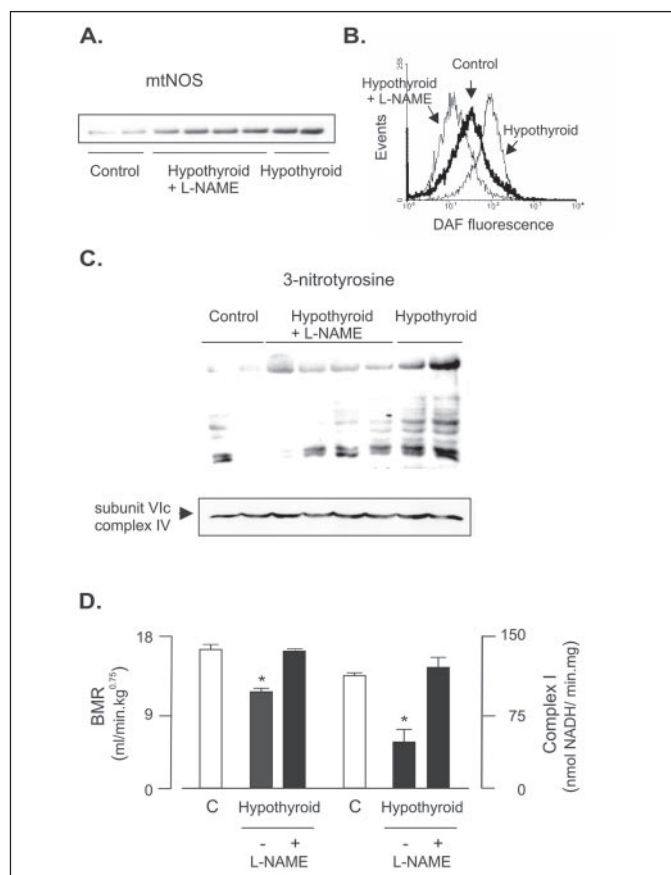he modulation of mtNOS activity and the putative regulation of cell cycle through redox signaling in the sequence of proliferating to quiescent cell stages during rat liver development (13).

In the same way, at the hypothyroid condition, liver P-p38MAPK was markedly expressed, whereas P-ERK1/2 and cyclin D1 mRNA and protein expression were very low (Fig. 5, *A* and *B*); the opposite pattern was detected after administration of T_3. In this context and regarding mtNOS-dependent redox changes, expression of cyclin D1 correlated with P-ERK1/2/P-p38 ratio that fitted well with experimentally measured mitochondrial $d[H_2O_2]/dt/d[NO]/dt$ (Fig. 5*C*), or with calculated $d[H_2O_2]/dt/d[ONOO^-]/dt$ ratios (not shown). Interestingly, concomitant administration of L-NAME to hypothyroid rats had the same effects on signaling as administration of T_3, without changing thyroid status.

DISCUSSION

This study shows, for the first time, that thyroid hormones modulate mRNA expression and subcellular distribution of nNOSα. As reported for eNOS subcellular traffic (34, 35), the translocation of nNOS to mitochondria could be influenced by regulation of posttranslational changes found in mitochondrial nNOS, (*N*-acylation, Ser-1412 phosphorylation) or by the turnover of cytosol "anchoring" proteins, like Hsp90 (Fig. 1*F*), dystrophin (36), or caveolin-1 (37).
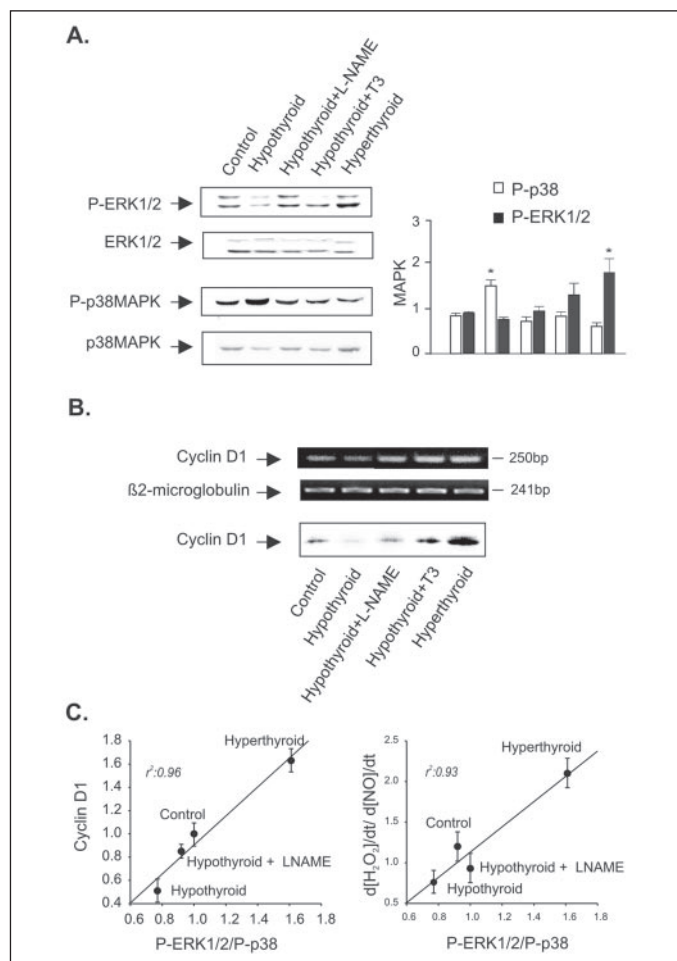
FIGURE 5. **Liver cell signaling depends on thyroid-dependent mitochondrial active species.** *A*, on the *left*, Western blots show differential activation of MAPKs of liver homogenates at different T_3 levels; on the *right*, densitometry of five separate experiments (for simplification, P-ERK is the sum of P-ERK1 and 2, at equal loading control). *B*, RT-PCR for cyclin D1 is compared with $\beta 2$-microglobulin, and Western blotting of cyclin D1 is included ($n = 5$). *C*, as a marker of liver proliferation rate at different thyroid status, cyclin expression correlates with P-ERK1/2/P-p38 ratio (*left*), which fits with experimentally measured mitochondrial $d[H_2O_2]/dt/d[NO]/dt$ ratio (Figs. 2A and 1C); $d[H_2O_2]/dt$ was measured with 6 mM malate-glutamate as substrate. *, $p < 0.05$ compared with control by analysis of variance. Regressions are significant at $p < 0.05$ level.

The notion that spatial confinement is essential to NOS signaling (6, 38) is supported here by differential modulation of O_2 uptake and nNOS distribution, depending on thyroid status; this notion could be extended to other cell adaptive responses (15, 39). It is then surmised that mitochondrial import of nNOS contributes to the typical decrease of BMR in hypothyroidism; though liver represents 10–12% of BMR, a similar response was found in skeletal muscle that provides 20–50% of BMR (10). Otherwise, down-regulation of mtNOS enhances T_3 genomic and non-genomic effects on mitochondrial and systemic O_2 uptake (2, 3).

In the absence of T_3, the interaction between nNOS and complexes I and IV provides steric advantage to further increase O_2^- and H_2O_2 production rates. As shown here (Fig. 3B), and depending on NO and O_2^- fluxes, $ONOO^-$ formation leads to selective nitration or nitrosylation of complex I (40). Although constitutive nitration is detected in controls, extensive nitration of different subunits in hypothyroidism is parallel to the markedly reduced electron transfer between NADH and ubiquinol acceptor. A similar causality could be applied to reduced complex IV activity (41). In accord, Persichini *et al.* (42) recently reported that the direct interaction shown here between cytochrome oxidase and mtNOS proceeds through PDZ domains. Likewise, complex inhibition contrib-

utes to set down BMR (43) and to further increase production of O_2 species (Fig. 2D) and $ONOO^-$ and to perpetuate nitration itself. In addition, it was previously reported that nitrated proteins are prone to be degraded by the ubiquitin-proteasome system (44, 45). Thus, restoring basal nitration level after T_3 replacement (Fig. 3, *A* and *B*) required *de novo* protein synthesis during mitochondrial biogenesis or a "denitration" process (46). In this context, NO itself may increase mitochondrial biogenesis by cGMP-dependent activation of peroxisome proliferator-activated receptor-γ coactivator 1α that stimulates the transcription of nuclear-encoded mitochondrial proteins (47).

It is worth noting that the administration of L-NAME completely prevents the phenotypic changes induced by hypothyroidism (low BMR, decreased complex I activity, increased protein nitration) without changing hormonal status. Considering that L-NAME did not modify nNOS expression or subcellular distribution, its effects likely rely on the inhibition of NOS activity within mitochondria.

In recent years, some reports indicated mitochondrial redox contribution to the activation of MAPK cascades (48). In agreement, higher levels of phosphorylated p38MAPK could be consistent with kinase activation by high oxidant levels or by $ONOO^-$ itself produced in hypothyroidism (13, 49). Currently, P-p38 participates in cell cycle arrest and inhibition of cell proliferation, a hallmark of hypothyroidism (1), whereas low oxidative stress and low $ONOO^-$ in hyperthyroidism are associated here with liver ERK1/2 activation and cyclin D1 expression (13), a hallmark of tissue proliferation. A similar effect of L-NAME or T_3 in turning hypothyroid cell signaling back to control status indicates that differential P-ERK1/2/P-p38MAPK ratio and expression of cyclin D1 should depend not on thyroid hormones themselves but on the relative production of mitochondrial oxidants, NO and $ONOO^-$, at the different T_3 levels.

T_3-dependent targeting of nNOS to mitochondria provides a new insight into the pathophysiology of hypo- and hyperthyroid syndromes. The presented mechanisms may gain importance in other situations associated with complex I dysfunction, like Parkinson disease.

REFERENCES

1. Moro, L., Marra, E., Capuano, F., and Greco, M. (2004) *Endocrinology* **145,** 5121–5128
2. Scanlan, T. S., Suchland, K. L., Hart, M. E., Chiellini, G., Huang, Y., Kruzich, P. J., Frascarelli, S., Crossley, D. A., Bunzow, J. R., Ronca-Testoni, S., Lin, E. T., Hatton, D., Zucchi, R., and Grandy, D. K. (2004) *Nat. Med.* **10,** 638–642
3. Pillar, T. M., and Seitz, H. J. (1997) *Eur. J. Endocrinol.* **136,** 231–239
4. Liggett, S. B. (2004) *Nat. Med.* **10,** 582–583
5. Toft, A. D. (1994) *New Engl. J. Med.* **331,** 171–180
6. Barouch, L. A., Harrison, R. W., Skaf, M. W., Rosas, G. O., Cappola, T. P., Kobeissi, Z. A., Hobai, I. A., Lemmon, C. A., Burnett, A. L., O'Rourke, B., Rodriguez, E. R., Huang, P. L., Lima, J. A., Berkowitz, D. E., and Hare, J. M. (2002) *Nature* **416,** 337–339
7. Fulton, D., Babbitt, R., Zoellner, S., Fontana, J., Acevedo, L., McCabe, T. J., Iwakiri, Y., and Sessa, W. C. (2004) *J. Biol. Chem.* **279,** 30349–30357
8. Giulivi, C., Poderoso, J. J., and Boveris, A. (1998) *J. Biol. Chem.* **273,** 11038–11043
9. Ghafourifar, P., and Cadenas, E. (2005) *Trends Pharmacol. Sci.* **26,** 190–195
10. Carreras, M. C., Peralta, J. G., Converso, D. P., Finocchietto, P. V., Rebagliati, I., Zaninovich, A. A., and Poderoso, J. J. (2001) *Am. J. Physiol.* **281,** H2282-H2288
11. Ghafourifar, P., Schenk, U., Klein, S. D., and Richter, C. (1999) *J. Biol. Chem.* **274,** 31185–31188
12. Elfering, S. L., Haynes, V. L., Traaseth, N. J., Ettl, A., and Giulivi, C. (2004) *Am. J. Physiol.* **286,** H22-H29
13. Carreras, M. C., Converso, D. P., Lorenti, A. S., Barbich, M., Levisman, D. M., Jaitovich, A., Antico Arciuch, V. G., Galli, S., and Poderoso, J. J. (2004) *Hepatology* **40,**

157–166

14. Riobo, N. A., Melani, M., Sanjuan, N., Fiszman, M. L., Gravielle, M. C., Carreras, M. C., Cadenas, E., and Poderoso, J. J. (2002) *J. Biol. Chem.* **277,** 42447–42455

15. Peralta, J. G., Finocchietto, P. V., Converso, D., Schopfer, F., Carreras, M. C., and Poderoso, J. J. (2003) *Am. J. Physiol.* **284,** H2375-H2383

16. Valdez, L. B., Zaobornyj, T., Alvarez, S., Bustamante, J., Costa, L. E., and Boveris, A. (2004) *Mol. Aspects Med.* **25,** 49–59

17. Brookes, P. S., Kraus, D. W., Shiva, S., Doeller, J. E., Barone, M. C., Patel, R. P., Lancaster, J. R., Jr., and Darley-Usmar, V. (2003) *J. Biol. Chem.* **278,** 31603–31609

18. Poderoso, J. J., Carreras, M. C., Lisdero, C., Riobo, N., Schopfer, F., and Boveris, A. (1996) *Arch. Biochem. Biophys.* **328,** 85–92

19. Poderoso, J. J., Lisdero, C., Schopfer, F., Riobo, N., Carreras, M. C., Cadenas, E., and Boveris, A. (1999) *J. Biol. Chem.* **274,** 37709–37716

20. Bianchi, M. S., Catalano, P. N., Bonaventura, M. M., Silveyra, P., Bettler, B., Libertun, C., and Lux-Lantos, V. A. (2004) *Neuroendocrinology* **80,** 129–142

21. Cymeryng, C. B., Lotito, S. P., Colonna, C., Finkielstein, C., Pomeraniec, Y., Grión, N., Gadda, L., Maloberti, P., and Podestá, E. J. (2002) *Endocrinology* **143,** 1235–1242

22. Alvarez, M., Depino, A. M., Podhajcer, O. L., and Pitossi, F. J. (2000) *Anal. Biochem.* **287,** 87–94

23. Ogilvie, P., Achilling, K., Billingsley, M. L., and Schmidt, H. (1995) *FASEB J.* **9,** 799–806

24. López-Figueroa, M., Caamaño, C., Morano, M. I., Ronn, L. C., Akil, H., and Watson, S. J. (2000) *Biochem. Biophys. Res. Commun.* **272,** 129–133

25. Berry, M. N., and Friend, D. S. (1969) *J. Cell Biol.* **43,** 506–520

26. Schägger, H. (2001) *Methods Cell Biol.* **65,** 231–244

27. Schagger, H., and von Jagow, G. (1991) *Anal. Biochem.* **199,** 223–231

28. Valdez, L. B., Zaobornyj, T., and Boveris, A. (2005) *Methods Enzymol.* **396,** 444–455

29. Venditti, P., De Rosa, R., and Di Meo, S. (2003) *Mol. Cell. Endocrinol.* **205,** 185–192

30. Lopez-Torres, M., Romero, M., and Barja, G. (2000) *Mol. Cell. Endocrinol.* **168,** 127–134

31. Das, K., and Chainy, G. B. (2001) *Biochim. Biophys. Acta* **1537,** 1–13

32. Myhre, O., Andersen, J. M., Aarnes, H., and Fonnum, F. (2003) *Biochem. Pharmacol.* **65,** 1575–1582

33. Pibiri, M., Ledda-Columbano, G. M., Cossu, C., Simbula, G., Menegazzi, M., Shinozuka, H., and Columbano, A. (2001) *FASEB J.* **15,** 1006–1013

34. Jiang, J., Cyr, D., Babbitt, R. W., Sessa, W. C., and Patterson, C. (2003) *J. Biol. Chem.* **278,** 49332–49341

35. Liu, J., Garcia-Cardena, G., and Sessa, W. C. (1995) *Biochemistry* **34,** 12333–12340

36. Kanai, A. J., Pearce, L. L., Clemens, P. R., Birder, L. A., VanBibber, M. M., Choi, S. Y., de Groat, W. C., and Peterson, J. (2001) *Proc. Natl. Acad. Sci. U. S. A.* **98,** 14126–14131

37. Sato, Y., Sagami, I., and Shimizu, T. (2004) *J. Biol. Chem.* **279,** 8827–8836

38. Hare, J. M. (2004) *Lancet* **363,** 1338–1339

39. Venkatraman, A., Shiva, S., Wigley, A., Ulasova, E., Chhieng, D., Bailey, S. M., and Darley-Usmar, V. M. (2004)) *Hepatology* **40,** 565–573

40. Riobo, N. A., Clementi, E., Melani, M., Boveris, A., Cadenas, E., Moncada, S., and Poderoso, J. J. (2001) *Biochem. J.* **359,** 139–145

41. Zhang, J., Jin, B., Li, L., Block, E. R., and Patel, J. M. (2005) *Am. J. Physiol.* **288,** C840-C849

42. Persichini, T., Mazzone, V., Polticelli, F., Moreno, S., Venturini, G., Clementi, E., and Colasanti, M. (2005) *Neurosci. Lett.* **384,** 254–259

43. Barrientos, A., and Moraes, C. T. (1999) *J. Biol. Chem.* **274,** 16188–16197

44. Souza, J. M., Choi, I., Chen, Q., Weisse, M., Daikhin, E., Yudkoff, M., Obin, M., Ara, J., Horwitz, J., and Ischiropoulos, H. (2000) *Arch. Biochem. Biophys.* **380,** 360–366

45. Carreras, M. C., Franco, M. C., Peralta, J. G., and Poderoso, J. J. (2004) *Mol. Aspects Med.* **25,** 125–139

46. Koeck, T., Fu, X., Hazen, S. L., Crabb, J. W., Stuehr, D. J., and Aulak, K. S. (2004) *J. Biol. Chem.* **279,** 27257–27262

47. Nisoli, E., Clementi, E., Paolucci, C., Cozzi, V., Tonello, C., Sciorati, C., Bracale, R., Valerio, A., Francolini, M., Moncada, S., and Carruba, M. O. (2003) *Science* **299,** 896–899

48. Dougherty, C. J., Kubasiak, L. A., Frazier, D. P., Li, H., Xiong, W. C., Bishopric, N. H., and Webster, K. A. (2004) *FASEB J.* **18,** 1060–1070

49. Jope, R. S., Zhang, L., and Song, L. (2000) *Arch. Biochem. Biophys.* **376,** 365–370

María C. Franco, Valeria G. Antico Arciuch, Jorge G. Peralta, Soledad Galli, Damián Levisman, Lidia M. López, Leonardo Romorini, Juan J. Poderoso and María C. Carreras

Access the most updated version of this article at doi: 10.1074/jbc.M512080200

Find articles, minireviews, Reflections and Classics on similar topics on the JBC Affinity Sites.

Alerts:

- When this article is cited
- When a correction for this article is posted

Click here to choose from all of JBC's e-mail alerts

This article cites 49 references, 17 of which can be accessed free at
http://www.jbc.org/content/281/8/4779.full.html#ref-list-1